STATI

SIMULATING BIVARIATE STATIONARY PROCESSES WITH SCALE-SPECIFIC CHARACTERISTICS

Milan Bašta*

1. Introduction

In univariate analysis, wavelets are useful for studying the dynamics of a time series as a function of scale and time. In our paper, we will be predominantly interested in the *scale* aspect. A scale can be informally considered proportional to the reciprocal of frequency with long scales (i.e., low frequencies) being associated with the long-term behavior of the time series and short scales (i.e., high frequencies) with abrupt changes. A time series can generally exhibit different variability at different scales. For example, it can be highly variable at short scales with its dynamics consisting of prominent abrupt changes, jumps, etc. Alternatively, it can be highly variable at long scales exhibiting noticeable trends and long-term patterns. We will call the characteristics that capture the variability of a time series across scales *scale-specific characteristics of variability*. One well-known scale-specific characteristics of variability is wavelet variance (see, e.g., Percival and Walden, 2002, Chapter 8).

In case of bivariate analysis, wavelets are suitable for exploring *scale-specific relationships*, i.e., relationships that change across scales. Tools suitable for studying scale-specific relationships include wavelet covariance, wavelet correlation, wavelet cross-covariance and wavelet cross-correlation (see, e.g., Percival and Walden, 2002; Whitcher et al., 1999; Whitcher et al., 2000; Serroukh and Walden, 2000a and 2000b). These tools have already been used in finance and economics. Ramsey and Lampart (1998a) and Ramsey and Lampart (1998b) studied the relationship between money and income and between expenditure and income, respectively. Atkins and Sun (2003) used wavelets to explore the relationship between interest rates and inflation and Gençay et

* University of Economics in Prague, Faculty of Informatics and Statistics (milan.basta@vse.cz).
This paper was written with the support of the Czech Science Foundation (GA CR), grant no. P402/12/P507, Modelling of Financial and Economic Time Series – Application and Comparison of Wavelet and Traditional Methods.

al. (2005) employed wavelets to explore relationships between the return of a portfolio and its beta. The results of these papers suggest that wavelets can be useful for revealing the nature of association between economic and financial time series.

In this paper, we deal with a related problem, namely how to build models of univariate and bivariate time series with prescribed scale-specific characteristics of variability and scale-specific relationships. In the univariate case of generating a single time series with prescribed scale-specific characteristics of variability, we modify the approach of Percival and Walden (2002, Section 9.2), which builds upon Wornell (1993 and 1996) and McCoy and Walden (1996). Afterwards, we suggest a way how this approach might be extended to the bivariate case of generating a pair of time series with prescribed scale-specific relationships. We find the formulas for the traditional autocovariance and cross-covariance sequences of the simulated bivariate process.

Related methodologies for simulating time series with scale-specific characteristics have already appeared in the literature; see, for example, Nason et al. (2000) and Sanderson et al. (2010). The relation of these methodologies to our approach will be discussed in Section 7.

Our paper is organized as follows. In Section 2, we define the discrete wavelet transform. In Section 3, we introduce the notion of wavelet variance, wavelet covariance and wavelet correlation. In Section 4, we modify the approach of Percival and Walden (2002, Section 9.2) and present a methodology for simulating univariate time series with scale-specific characteristics of variability. In Section 5, we generalize the methodology to the case of simulating bivariate time series with prescribed scale-specific relationships. In Section 6, Monte Carlo simulation is used to verify that our methodology works well. Section 7 compares our models to the models of Nason et al. (2000) and Sanderson et al. (2010). Section 8 concludes, pointing out the relevance of our approach to financial time series.

2. The discrete wavelet transform

Our introduction to the discrete wavelet transform (DWT) is based on Percival and Walden (2002).

2.1 The DWT

Let us assume a real-valued time series $\{X_t: t = 0, 1, \ldots, N - 1\}$ of length N, where $N = 2^J$, J being a positive integer. This restriction on the length of the time series is necessary for defining the DWT. Let $\mathbf{X}$ be an N-dimensional vector consisting of the values of the time series $\{X_t\}$, the first element of $\mathbf{X}$ being X_0, the second X_1, etc. $\mathbf{X}$ can be considered a random vector since the time series can be considered a portion of length N of a real-valued discrete-time stochastic process.

The *DWT* of **X** is defined as

$$\mathbf{W} \equiv \Omega\mathbf{X}, \tag{1}$$

where **W** is a real-valued N-dimensional vector of the *DWT coefficients*. Ω is an $N \times N$ non-random real-valued orthonormal matrix, which defines the DWT. The elements of Ω are fully determined if the length of the time series, $N = 2^J$, and the type of wavelets (e.g., Haar, Daubechies, coiflet etc.) used in the analysis are given. For example, for $N = 2^3 = 8$ and Haar wavelets, Ω is given as

$$\Omega_{Haar} \equiv \begin{bmatrix} -\frac{1}{\sqrt{2}} & \frac{1}{\sqrt{2}} & 0 & 0 & 0 & 0 & 0 & 0 \\ 0 & 0 & -\frac{1}{\sqrt{2}} & \frac{1}{\sqrt{2}} & 0 & 0 & 0 & 0 \\ 0 & 0 & 0 & 0 & -\frac{1}{\sqrt{2}} & \frac{1}{\sqrt{2}} & 0 & 0 \\ 0 & 0 & 0 & 0 & 0 & 0 & -\frac{1}{\sqrt{2}} & \frac{1}{\sqrt{2}} \\ -\frac{1}{2} & -\frac{1}{2} & \frac{1}{2} & \frac{1}{2} & 0 & 0 & 0 & 0 \\ 0 & 0 & 0 & 0 & -\frac{1}{2} & -\frac{1}{2} & \frac{1}{2} & \frac{1}{2} \\ -\frac{1}{\sqrt{8}} & -\frac{1}{\sqrt{8}} & -\frac{1}{\sqrt{8}} & -\frac{1}{\sqrt{8}} & \frac{1}{\sqrt{8}} & \frac{1}{\sqrt{8}} & \frac{1}{\sqrt{8}} & \frac{1}{\sqrt{8}} \\ \frac{1}{\sqrt{8}} & \frac{1}{\sqrt{8}} & \frac{1}{\sqrt{8}} & \frac{1}{\sqrt{8}} & \frac{1}{\sqrt{8}} & \frac{1}{\sqrt{8}} & \frac{1}{\sqrt{8}} & \frac{1}{\sqrt{8}} \end{bmatrix}. \tag{2}$$

In general, Ω can be partitioned into $J + 1$ matrices $\Omega_1, \Omega_2, \ldots, \Omega_J, \Theta_J$ as follows:

$$\Omega = \begin{bmatrix} \Omega_1 \\ \Omega_2 \\ \vdots \\ \Omega_J \\ \Theta_J \end{bmatrix}, \tag{3}$$

where the size of Ω_j (for $j = 1, 2, \ldots, J$) is $N_j \times N$, where

$$N_j \equiv \frac{N}{2^j}, \tag{4}$$

and the size of Θ_J is $1 \times N$. The $(r+1)$th (for $r = 1, \ldots, N_j - 1$) row of Ω_j is the rth row of Ω_j circularly shifted by 2^j units. The partitioning of Ω implies the following partitioning of $\mathbf{W}$ into $J+1$vectors $\mathbf{W}_1, \mathbf{W}_2, \ldots, \mathbf{W}_J, \mathbf{V}_J$:

$$\mathbf{W} = \begin{bmatrix} \mathbf{W}_1 \\ \mathbf{W}_2 \\ \vdots \\ \mathbf{W}_J \\ \mathbf{V}_J \end{bmatrix}, \tag{5}$$

where $\mathbf{W}_j \equiv \Omega_j \mathbf{X}$ (for $j = 1, 2, \ldots, J$) is an N_j-dimensional vector of the *jth level wavelet coefficients*, and $\mathbf{V}_J = \Theta_J \mathbf{X}$ is a one-dimensional vector consisting of a single *Jth level scaling coefficient*. The elements of $\mathbf{W}_j$ (for $j = 1, 2, \ldots, J$) are (for many types of wavelets) associated with *changes* of (weighted) averages of the input time series ($\mathbf{X}$), these averages being calculated at scale 2^{j-1}. $\mathbf{V}_J$, on the other hand, has a different meaning: it is associated with the average of the input time series calculated at scale 2^J.

2.2 The DWT and linear filtering

The DWT coefficients can also be obtained as a result of circular filtering the time series $\{X_t: t = 0, 1, \ldots, N-1\}$ with a special set of $J+1$ filters and via subsampling of the result subsequently. The $J+1$ filters are denoted as $\{h_{1,t}: t = 0, \ldots, L_1 - 1\}$, $\{h_{2,t}: t = 0, \ldots, L_2 - 1\}$, ..., $\{h_{J,t}: t = 0, \ldots, L_J - 1\}$ and $\{g_{J,t}: t = 0, \ldots, L_J - 1\}$, where $L_1, L_2, \ldots, L_J$ are the lengths of these filters. The length L_j (for $j = 2, \ldots, J$) is related to the length L_1 as

$$L_j = (2^j - 1)(L_1 - 1) + 1. \tag{6}$$

The exact values of these $J+1$ filters are fully determined by the type of wavelets used in the analysis and are directly related to the elements of Ω.

Now, let us express $\mathbf{W}_j$ (for $j = 1, 2, \ldots, J$) and $\mathbf{V}_J$ as

$$\mathbf{W}_j = [W_{j,0}, W_{j,1}, \ldots, W_{j,N_j-1}]^T, \qquad \mathbf{V}_J = \left[V_{J,0}\right], \tag{7}$$

where $W_{j,t}$ (for $t = 0, \ldots, N_j - 1$) is the $(t + 1)$th element of $\mathbf{W}_j$ and $V_{J,0}$ is the only element of $\mathbf{V}_J$. We can write

$$W_{j,t} = \sum_{l=0}^{L_j - 1} h_{j,l} X_{2^j (t+1) - 1 - l \bmod N}, \text{ for } j = 1, \ldots, J, t = 0, \ldots, N_j - 1, \tag{8}$$

$$V_{J,0} = \sum_{l=0}^{L_j - 1} g_{J,l} X_{2^j - 1 - l \bmod N}, \tag{9}$$

where "mod" denotes the operation modulo. Equations 8 and 9 imply that the elements of $\mathbf{W}_j$ (for $j = 1, \ldots, J$) and $\mathbf{V}_J$ can be obtained via circular filtering of $\{X_t\}$ with $\{h_{j,t}\}$ and $\{g_{J,t}\}$, respectively, and via the consequent subsampling of the result by 2^j and 2^J, respectively.

$\{h_{j,t}\}$ (for $j = 1, \ldots, J$) approximates a band-pass filter with the nominal pass band $[2^{-(j+1)}, 2^{-j}]$. As a result, $\mathbf{W}_j$ is associated with the dynamics of the input time series in the frequency range $[2^{-(j+1)}, 2^{-j}]$. Analogously, $\{g_{J,t}\}$ is approximately a low-pass filter with the nominal pass band $[0, 2^{-(J+1)}]$ and thus $\mathbf{V}_J$ is associated with the dynamics of the input time series in the range of frequencies $[0, 2^{-(J+1)}]$.

Those elements of $\mathbf{W}_j$ (for $j = 1, \ldots, J$) for which the omission of the modulo operation in Equation 8 would lead to the coefficients not being properly defined, are called *boundary coefficients*. The value of the boundary coefficients is affected by the assumption inherent in Equation 8, namely the fact that the input time series is treated as if it was periodic with the period equal to N, the values preceding X_0 being X_{N-1}, X_{N-2} etc. Since this assumption is often unrealistic in practical settings, boundary coefficients are often excluded from further analysis. As documented in Percival and Walden (2002, pages 136 and 146), the first

$$\min\left(N_j, ceiling((L_1 - 2)(1 - 1/2^j))\right) \tag{10}$$

coefficients of $\mathbf{W}_j$ (for $j = 1, \ldots, J$) are boundary coefficients (*ceiling*(b) is defined as the smallest integer greater than or equal to b). The remaining coefficients of $\mathbf{W}_j$ are called *non-boundary coefficients*. Similarly, the coefficient $V_{J,0}$ of Equation 9 will be treated as boundary in our paper if the modulo operation cannot be left out of its definition.

2.3 The DWT of an infinite portion of a stochastic process

Now, let us modify Equations 8 and 9 in such a way that $\{h_{j,t}\}$ (for $j = 1, \ldots, J$) and $\{g_{J,t}\}$ are applied to the process $\{X_t: t = \ldots, -1, 0, 1, \ldots\}$ and not to a finite portion thereof as was the case in Equations 8 and 9. Then, we can write

$$w_{j,t} \equiv \sum_{l=0}^{L_j-1} h_{j,l} X_{2^j(t+1)-1-l}, \text{ for } j = 1,...,J, t = ...,-1,0,1.... \quad (11)$$

$$v_{J,t} \equiv \sum_{l=0}^{L_J-1} g_{J,l} X_{2^j(t+1)-1-l}, \text{ for } t = ...,-1,0,1,... \quad (12)$$

The results are denoted as $\{w_{j,t}: t = \ldots, -1, 0, 1, \ldots\}$ and $\{v_{J,t}: t = \ldots, -1, 0, 1, \ldots\}$ in order to distinguish them from $\{W_{j,t}: t = 0, \ldots, N_j - 1\}$ and $\{W_{j,t}: t = 0\}$, which were the results of circular filtering of $\{X_t: t = 0, 1, \ldots, N-1\}$ with $\{h_{j,t}\}$ and $\{g_{J,t}\}$. If $\{X_t: t = \ldots, -1, 0, 1, \ldots\}$ is stationary, $\{w_{j,t}: t = \ldots, -1, 0, 1, \ldots\}$ (for $j = 1, ..., J$) and $\{v_{J,t}: t = \ldots, -1, 0, 1, \ldots\}$ are obviously stationary, too.

2.3 Inverse DWT

The DWT is an orthonormal transform which implies that the inverse DWT can be written as

$$\mathbf{X} = \Omega^{-1}\mathbf{W} = \Omega^T\mathbf{W}. \quad (13)$$

Making use of the partitioning of Ω and $\mathbf{W}$ described in Section 2.1, the matrix multiplication of Equation 13 can be rewritten as

$$\mathbf{X} = \Omega^T\mathbf{W} = \sum_{j=1}^{J} \Omega_j^T\mathbf{W}_j + \Theta_J^T\mathbf{V}_J. \quad (14)$$

Equation 14 implies that the input time series ($\mathbf{X}$) can be synthesized from the DWT coefficients ($\mathbf{W}$). The term $\Omega_j^T\mathbf{W}_j$ might be considered the contribution of scale 2^{j-1} to this synthesis.

3. Wavelet covariance, variance and correlation

In the next paragraphs, we introduce the notions of wavelet and scaling covariance (Section 3.1) and wavelet and scaling correlation (Section 3.4), which are helpful for exploring scale-specific relationships between a pair of processes. Wavelet and scaling variances that can be utilized for exploring scale-specific characteristics of variability of a single process are introduced in Section 3.3.

3.1 Wavelet and scaling covariance

Let us assume two real-valued time series $\{X_t: t = 0, 1, \ldots, N-1\}$ and $\{Y_t: t = 0, 1, \ldots, N-1\}$, both of a length $N = 2^J$, J being a positive integer. Let these time series be portions of length N of two zero-mean components, $\{X_t: t = \ldots, -1, 0, 1, \ldots\}$ and

$\{Y_t: t = \dots, -1, 0, 1, \dots\}$, of a real-valued bivariate discrete-time stochastic process. Let the *cross-covariance* sequence between the components of the bivariate process be defined as

$$s_{XY,\tau} \equiv \mathrm{cov}(X_t, Y_{t+\tau}) = E\left(X_t Y_{t+\tau}\right) \quad \text{for } \tau = ..., -1, 0, 1..., \tag{15}$$

where τ is the lag. Let the *cross-spectrum* between the components be defined as the Fourier transform of $\{s_{XY,\tau}: \tau = \dots, -1, 0, 1, \dots\}$, i.e.,

$$S_{XY}(f) \equiv \sum_{\tau=-\infty}^{\infty} s_{XY,\tau} \exp(-i2\pi f \tau), \quad \text{for } f \in R, \tag{16}$$

where i is the imaginary unit and f is a real-valued non-random variable called *frequency*. In this paper, the cross-covariance sequence will always be assumed to be symmetric around zero. Under this assumption, the cross-spectrum is obviously a real--valued, even and periodic function of frequency with the period equal to unity. Taking the inverse Fourier transform of such a cross-spectrum, we get

$$s_{XY,\tau} = 2\int_0^{1/2} S_{XY}(f) \exp(+i2\pi f \tau) df, \quad \text{for } \tau = ..., -1, 0, 1, ... \tag{17}$$

Setting $\tau = 0$ in Equation 17, we obtain

$$s_{XY,0} = 2\int_0^{1/2} S_{XY}(f) df, \tag{18}$$

which implies that the cross-spectrum informs us about the contribution of different frequency bands to the covariance $s_{XY,0}$.

Let $\{X_t: t = \dots, -1, 0, 1, \dots\}$ and $\{Y_t: t = \dots, -1, 0, 1, \dots\}$ be the inputs into Equation 11, the outputs being denoted as $\{w_{X,j,t}: t = \dots, -1, 0, 1, \dots\}$ and $\{w_{Y,j,t}: t = \dots, -1, 0, 1, \dots\}$ (for $j = 1, \dots, J$), respectively. Let us define

$$C_{XY,j} \equiv \mathrm{cov}(w_{X,j,t}, w_{Y,j,t}), \quad \text{for } j = 1, ..., J. \tag{19}$$

The filtering theory implies that the cross-spectrum between $\{w_{X,j,t}: t = \dots, -1, 0, 1, \dots\}$ and $\{w_{Y,j,t}: t = \dots, -1, 0, 1, \dots\}$ is given as

$$S_{w_{X,j}w_{Y,j}}(f) = S_{XY}(f)\left|H_j(f)\right|^2, \quad \text{for } f \in R, \tag{20}$$

where

$$\left|H_j(f)\right|^2 \equiv \left|\sum_{t=0}^{L_j-1} h_{j,t} \exp(-i2\pi f t)\right|^2, \quad \text{for } f \in R, \text{ for } j = 1,...,J, \tag{21}$$

is the *squared gain function* of $\{h_{j,t}\}$. This squared gain function is a real-valued, even and periodic function with the period equal to unity. We can write (see Percival and Walden, 2002)

$$\left|H_j(f)\right|^2 \approx \begin{cases} 2^j, & f \in \left[2^{-(j+1)}, 2^{-j}\right] \\ 0, & f \in [0,1/2] \setminus \left[2^{-(j+1)}, 2^{-j}\right] \end{cases}, \quad \text{for } j = 1,...,J. \tag{22}$$

Making use of Equations 18, 20 and 22, we can thus write

$$C_{XY,j} = 2\int_0^{1/2} S_{w_{X,j}w_{Y,j}}(f)df = 2\int_0^{1/2} S_{XY}(f)\left|H_j(f)\right|^2 \approx 2\int_{1/2^{j+1}}^{1/2^j} 2^j S_{XY}(f)df. \tag{23}$$

Equation 23 implies that $C_{XY,j}/2^j$ (for $j = 1, \ldots, J$) can be approximately interpreted as the contribution of the range of frequencies $[2^{-(j+1)}, 2^{-j}]$ (or scale 2^{j-1}) to $s_{XY,0}$. This leads to the following definition of the *jth level wavelet covariance*,

$$\eta_{XY,j} \equiv \frac{C_{XY,j}}{2^j}, \text{ for } j = 1,...,J. \tag{24}$$

Analogously, let $\{v_{X,J,t}: t = \ldots, -1, 0, 1, \ldots\}$ and $\{v_{Y,J,t}: t = \ldots, -1, 0, 1, \ldots\}$ be the outputs of Equation 12 for the inputs $\{X_t: t = \ldots, -1, 0, 1, \ldots\}$ and $\{Y_t: t = \ldots, -1, 0, 1, \ldots\}$. We can write

$$B_{XY,j} \equiv \text{cov}(v_{X,j,t}, v_{Y,j,t}), \quad \text{for } t = ...,-1,0,1,... \tag{25}$$

$$B_{XY,J} \approx 2\int_0^{1/2^{J+1}} 2^J S_{XY}(f)df. \tag{26}$$

$B_{XY,J}/2^J$ can be (at least approximately) interpreted as the contribution of the range

of frequencies $[0, 2^{-(J+1)}]$ to $s_{XY,0}$. This leads to the definition of the *Jth level scaling covariance*,

$$\xi_{XY,J} \equiv \frac{B_{XY,J}}{2^J}. \tag{27}$$

Further, $s_{XY,0}$ can be decomposed as (see Serroukh and Walden, 2000a)

$$s_{XY,0} = \xi_{XY,J} + \sum_{j=1}^{J} \eta_{XY,j}. \tag{28}$$

3.2 Cross-covariance matrix of the DWT coefficients

Let the values of the time series $\{X_t: t = 0, 1, \ldots, N-1\}$ and $\{Y_t: t = 0, 1, \ldots, N-1\}$ be stacked into two N-dimensional zero-mean vectors denoted as $\mathbf{X}$ and $\mathbf{Y}$. The cross--covariance matrix $\Sigma_{\mathbf{XY}}$ between $\mathbf{X}$ and $\mathbf{Y}$ is a symmetric Toeplitz matrix given as

$$\Sigma_{\mathbf{XY}} \equiv E(\mathbf{X}\mathbf{Y}^T). \tag{29}$$

Let $\mathbf{W}_\mathbf{X} \equiv \Omega\mathbf{X}$ and $\mathbf{W}_\mathbf{Y} \equiv \Omega\mathbf{Y}$ be the DWT coefficients of $\mathbf{X}$ and $\mathbf{Y}$. The cross-covariance matrix between $\mathbf{W}_\mathbf{X}$ and $\mathbf{W}_\mathbf{Y}$ is given as

$$\Psi_{\mathbf{XY}} \equiv E\left(\mathbf{W}_\mathbf{X}\mathbf{W}_\mathbf{Y}^T\right) = \Omega\Sigma_{\mathbf{XY}}\Omega^T. \tag{30}$$

Let us stack the diagonal of this matrix into an N-dimensional vector $\mathbf{P}$, which can be partitioned into $J+1$ vectors $\mathbf{P}_1, \mathbf{P}_2, \ldots, \mathbf{P}_J, \mathbf{Q}_J$ in the following way:

$$\mathbf{P} = \begin{bmatrix} \mathbf{P}_1 \\ \mathbf{P}_2 \\ \vdots \\ \mathbf{P}_J \\ \mathbf{Q}_J \end{bmatrix}, \tag{31}$$

where $\mathbf{P}_j$ (for $j = 1, \ldots, J$) is an N_j-dimensional vector and $\mathbf{Q}_J$ one-dimensional. Those elements of $\mathbf{P}_j$ (for $j = 1, \ldots, J$) which are associated with non-boundary coefficients of $\mathbf{W}_{\mathbf{X},j}$ and $\mathbf{W}_{\mathbf{Y},j}$ (where $\mathbf{W}_{\mathbf{X},j} \equiv \Omega_j\mathbf{X}$ and $\mathbf{W}_{\mathbf{Y},j} \equiv \Omega_j\mathbf{Y}$) are obviously all the same and

equal to $C_{XY,j} = 2^j \eta_{XY,j}$. If the only element of $\mathbf{Q}_J$ is also associated with non-boundary coefficients, its value is obviously equal to $B_{XY,J} = 2^J \xi_{XY,J}$.

Following a similar line of argument to that of Percival and Walden (2002, p. 348), we can argue that two requirements need to be met so that the off-diagonal elements $\Psi_{\mathbf{XY}}$ are approximately zero. Firstly, we have to require that $\{h_{1,t}\}$, $\{h_{2,t}\}$, ..., $\{h_{J,t}\}$ and $\{g_{J,t}\}$ be band-pass filters for different (i.e., non-overlapping) pass bands. This requirement is approximately fulfilled as has already been stated in Section 2.2. Secondly, the cross-spectrum $S_{XY}(.)$ must be approximately constant in each of the following ranges of frequencies: $[2^{-2}, 2^{-1}]$, $[2^{-3}, 2^{-2}]$, ..., $[2^{-(J+1)}, 2^{-J}]$ and $[0, 2^{-(J+1)}]$. Even though this assumption is not met in general, it might be assumed to be valid for many real-life bivariate processes.

3.3 Univariate characteristics, wavelet and scaling variance

If we substitute $\{X_t: t = \dots, -1, 0, 1, \dots\}$ for $\{Y_t: t = \dots, -1, 0, 1, \dots\}$, Equations 15, 16, 24 and 27 will provide definitions of the autocovariance sequence, $\{s_{XX,\tau}: \tau = \dots, -1, 0, 1, \dots\}$, the spectrum, $S_{XX}(.)$, the *jth level wavelet variance*, $\eta_{XX,j}$, and the *Jth level scaling variance*, $\xi_{XX,J}$, of $\{X_t: t = \dots, -1, 0, 1, \dots\}$. Additionally, $\Sigma_{\mathbf{XY}}$ will become the covariance matrix of $\mathbf{X}$, $\Sigma_{\mathbf{XX}}$. Based on $\Sigma_{\mathbf{XX}}$, we may obtain the matrix $\Psi_{\mathbf{XX}}$, whose off-diagonal elements are close to zero for many types of processes (see Percival and Walden, 2002, Chapter 9; Vidakovic, 1999).

By the same token, if we substitute $\{Y_t: t = \dots, -1, 0, 1, \dots\}$ for $\{X_t: t = \dots, -1, 0, 1, \dots\}$ in the definitions of Sections 3.1 and 3.2, we get analogous univariate quantities for $\{Y_t: t = \dots, -1, 0, 1, \dots\}$, denoted as $\{s_{YY,\tau}: \tau = \dots, -1, 0, 1, \dots\}$, $S_{YY}(.)$, $\eta_{YY,j}$, $\xi_{YY,J}$, $\Sigma_{\mathbf{YY}}$ and $\Psi_{\mathbf{YY}}$.

3.4 Wavelet and scaling correlation

The *jth level wavelet correlation* $\rho_{XY,j}$ is defined as

$$\rho_{XY,j} \equiv \frac{\eta_{XY,j}}{\sqrt{\eta_{XX,j}}\sqrt{\eta_{YY,j}}}, \quad \text{for } j = 1,\dots,J. \tag{32}$$

The Jth level *scaling correlation* is defined as

$$\varphi_{XY,J} \equiv \frac{\eta_{XY,J}}{\sqrt{\eta_{XX,J}}\sqrt{\eta_{YY,J}}}. \tag{33}$$

4. Simulation of univariate stationary processes with prescribed wavelet and scaling variances

We introduce a way of simulating univariate processes with prescribed wavelet and scaling variances. The core of the methodology is given in Section 4.1, being a modification of the approach of Percival and Walden (2002, Section 9.2), which is based on the work of Wornell (1993 and 1996) and McCoy and Walden (1996). The modification lies in the fact that while Percival and Walden (2002, Section 9.2) aim at approximately simulating a long-memory process with a given spectrum using wavelets, we aim at exactly simulating a stationary process with prescribed wavelet and scaling variances. As a part of this modification, we have to solve a system of linear equations for a set of free parameters (see Section 4.3) to ensure that the simulated process has exactly the prescribed characteristics. We also derive a formula for the autocovariance sequence of the simulated process (Section 4.2), emphasizing that it consists of contributions of different scales.

4.1 Modification of the approach of Percival and Walden

$\Psi_{\mathbf{XX}}$ is approximately diagonal for many types of processes (see Section 3.3). Even though the uncorrelatedness of the components of $\mathbf{W}$ does not generally imply their independence, it can sometimes be the case (for example if $\mathbf{W}$ has a multivariate normal distribution). This offers an appealing way of simulating stationary processes with prescribed wavelet and scaling variances.

More specifically, let us simulate a portion, denoted as $\{X_t: t = 0, \ldots, 4N - 1\}$ (of a length $4N = 2^{J+2}$, J being a positive integer) of a zero-mean stationary process with wavelet variances $\eta_{XX,1}, \eta_{XX,2}, \ldots, \eta_{XX,J+2}$ and the $(J + 2)$th level scaling variance $\xi_{XX,J+2}$. Even though we simulate a portion of a length $4N$ in the first place, we will eventually use only the first N simulated values due to a reason which becomes obvious at the end of Section 4.4.

Step 1: Let $\alpha_{XX,1}, \alpha_{XX,2}, \ldots, \alpha_{XX,J+2}$ and $\beta_{XX,J+2}$ be non-negative real-valued parameters whose values are yet to be determined (Section 4.3). Let $\mathbf{U}$ be a $4N$-dimensional random vector whose components are $2N + N + N/2 + N/4 + \ldots + 1 + 1 = 4N$ independent zero-mean univariate random variables. The variances of the first $2N$ random variables (which constitute the vector $\mathbf{U}$) are set equal to $2^1\alpha_{XX,1}$. The variances of the next N random variables are set equal to $2^2\alpha_{XX,2}$. The variances of the next $N/2$, $N/4$, …, 1 random variables are set equal to $2^3\alpha_{XX,3}$, $2^4\alpha_{XX,4}, \ldots, 2^{J+2}\alpha_{XX,J+2}$. Finally, the last random variable, which constitutes the vector $\mathbf{U}$, has the variance set equal to $2^{J+2}\beta_{XX,J+2}$. $\mathbf{U}$ is called a *generating vector*.

Step 2: The inverse DWT of Equation 13 can be applied to $\mathbf{U}$, the result being $\Omega^T\mathbf{U}$.

Step 3: $\Omega^T\mathbf{U}$ encodes a portion of length $4N$ of a stochastic process, which we, among others, require to be stationary. However, this requirement is not met, because the autocovariance sequence of the portion of the stochastic process encoded in $\Omega^T\mathbf{U}$ is not constant in time (see Percival and Walden, 2002, p. 356). Percival and Walden (2002, p. 356) argue that stationarity can be achieved by applying a random circular shift to $\Omega^T\mathbf{U}$. More specifically, let the $4N \times 4N$ matrix Π be defined in the following way:

$$\Pi \equiv \begin{bmatrix} 0 & 0 & 0 & \cdots & 0 & 0 & 1 \\ 1 & 0 & 0 & \cdots & 0 & 0 & 0 \\ 0 & 1 & 0 & \cdots & 0 & 0 & 0 \\ 0 & 0 & 1 & \cdots & 0 & 0 & 0 \\ \vdots & \vdots & \vdots & \ddots & \vdots & \vdots & \vdots \\ 0 & 0 & 0 & \cdots & 1 & 0 & 0 \\ 0 & 0 & 0 & \cdots & 0 & 1 & 0 \end{bmatrix}. \tag{34}$$

The result of the random circular shift applied to $\Omega^T \mathbf{U}$ is a $4N$-dimensional vector defined as

$$\mathbf{X} \equiv \Pi^k \Omega^T \mathbf{U} = \Omega^T (\Omega \Pi^k \Omega^T) \mathbf{U}, \tag{35}$$

where k denotes a random variable distributed uniformly over integers 0, 1, …, $4N - 1$. It follows that the covariance matrix of $\mathbf{X}$ is given as

$$\Sigma_{\mathbf{XX}} \equiv \frac{1}{4N} \sum_{k=0}^{4N-1} \Pi^k \Omega^T \Sigma_{\mathbf{UU}} \Omega \left(\Pi^k\right)^T = circ\left(\Omega^T \Sigma_{\mathbf{UU}} \Omega\right), \tag{36}$$

where $\Sigma_{\mathbf{UU}}$ is the covariance matrix of $\mathbf{U}$ and *circ* is such an operator whose input can be any $(4N \times 4N)$ matrix Δ, the output being defined as

$$circ\,(\Delta) \equiv \frac{1}{4N} \sum_{k=0}^{4N-1} \Pi^k \Delta \left(\Pi^k\right)^T. \tag{37}$$

4.2 Obtaining the exact values of wavelet and scaling variances

Apart from being stationary, we require the simulated process to have wavelet variances equal to $\eta_{XX,1}$, $\eta_{XX,2}$, …, $\eta_{XX,J+2}$ and the $(J + 2)$th level scaling variance equal to $\xi_{XX,J+2}$. Making use of Equation 36 and the partitioning of Ω given in Equation 3, we can obtain

$$\Sigma_{\mathbf{XX}} = \sum_{j=1}^{J+2} 2^j \alpha_{XX,j}\, circ\,(\Omega_j^T \Omega_j) + 2^{J+2} \beta_{XX,J+2}\, circ\,(\Theta_{J+2}^T \Theta_{J+2}), \tag{38}$$

which implies that $\Sigma_{\mathbf{XX}}$ is a sum of several matrices each associated with a different scale. Further, let $\Omega_i \mathbf{X}$ (for $i = 1, \ldots, J + 2$) be the vector of the ith level wavelet coefficients of $\mathbf{X}$ and let $\Gamma_i = \Omega_i \Sigma_{\mathbf{XX}} \Omega_i^T$ be the covariance matrix of $\Omega_i \mathbf{X}$. It follows that

$$\Gamma_i = \sum_{j=1}^{J+2} 2^j \alpha_{XX,j} \Omega_i circ(\Omega_j^T \Omega_j) \Omega_i^T + 2^{J+2} \beta_{XX,J+2} \Omega_i circ(\Theta_{J+2}^T \Theta_{J+2}) \Omega_i^T . \quad (39)$$

Γ_i is a circulant matrix since $\Sigma_{\mathbf{XX}}$ is a circulant matrix (see Equation 36) and the $(r+1)$th (for $r = 1, \ldots, 4N/2^i - 1$) row of Ω_i is the rth row of W_i circularly shifted by an amount 2^i (see Section 2.1). Consequently, the diagonal of Γ_i (for $i = 1, \ldots, J+2$) is constant and is determined by one single number, which we require to be equal to $2^i \eta_{XX,i}$. Now, there are $(J+3)$ parameters $\alpha_{XX,1}$, $\alpha_{XX,2}$, …, $\alpha_{XX,J+2}$ and $\beta_{XX,J+2}$, which determine the value of the diagonal of Γ_i (see Equation 39). However, the total number of matrices Γ_i is $J+2$, because i runs over integers from 1 through $J+2$. Moreover, there is one additional covariance matrix, corresponding to the $(J+2)$th level scaling coefficients of **X**, whose diagonal is constant and required to be equal to $2^{J+2} \xi_{XX,J+2}$. All together, we thus have $(J+3)$ linear equations for $(J+3)$ unknown parameters $\alpha_{XX,1}$, $\alpha_{XX,2}$, …, $\alpha_{XX,J+2}$ and $\beta_{XX,J+2}$. If we solve for these parameters and if all are non-negative, then they are valid inputs into step 1 of Section 4.1 and lead to exact simulation with the required wavelet and scaling variances.

4.3 The autocovariance sequence

The autocovariance sequence of $\{X_t: t = 0, \ldots, 4N-1\}$, denoted as $\{s_{XX,\tau}: \tau = -(4N-1), \ldots, 0, \ldots, (4N-1)\}$, can be extracted from $\Sigma_{\mathbf{XX}}$ in the following way:

$$s_{XX,\tau} \equiv \begin{cases} \Sigma_{\mathbf{XX},|\tau|+1,1} & \text{for } \tau = -(4N-1), \ldots, -1, \\ \Sigma_{\mathbf{XX},1,\tau+1} & \text{for } \tau = 0, \ldots, (4N-1), \end{cases} \quad (40)$$

where $\Sigma_{\mathbf{XX},m,n}$ denotes the element of the matrix $\Sigma_{\mathbf{XX}}$ in the mth row and the nth column.

4.4 Symmetry of the autocovariance sequence

X might be considered a realization of a stationary stochastic process $\{X_t: t = 0, \ldots, 4N-1\}$. Since $\Sigma_{\mathbf{XX}}$ is a circulant matrix, the autocovariance sequence of $\{X_t: t = 0, \ldots, 4N-1\}$ is symmetric around the lag $\tau = 4N/2$. To avoid this undesirable property, we apply the suggestion of Percival and Walden (2002, p. 357) and use only the first N simulated values (out of the total number $4N$) for the final output. Thus, if the simulated time series is required to have the length N at the output, we have to simulate $4N$ values in the first place.

5. Simulation of bivariate stationary processes with prescribed wavelet and scaling variances/correlations

In this section, we propose a generalization of the methodology presented in Section 4 to the bivariate case. The two components that constitute the bivariate process that we want to simulate will comove, the nature of the comovement being different on different scales. By construction, the cross-covariance sequence between the components will be symmetric around zero.

5.1 Methodology

Let us simulate portions $\{X_t: t = 0, \ldots, 4N - 1\}$ and $\{Y_t: t = 0, \ldots, 4N - 1\}$, both of a length $4N = 2^{J+2}$, of two zero-mean components of a real-valued bivariate stationary process. Even though $4N$ values of each component are simulated in the first place, we will use only the first N simulated values in the end (because of the argument of Section 4.4). Let the jth level (for $j = 1, \ldots, J + 2$) wavelet variance of the first and second component (of the bivariate process) be denoted as $\eta_{XX,j}$ and $\eta_{YY,j}$, respectively. Similarly, let the $(J + 2)$th level scaling variances of the components be denoted as $\xi_{XX,J}$ and $\xi_{YY,J}$, respectively. Moreover, let the first through the $(J + 2)$th level wavelet correlations and the $(J + 2)$th level scaling correlation between the components be denoted as $\rho_{XY,1}, \rho_{XY,2}, \ldots, \rho_{XY,J}$ and $\varphi_{XY,J}$.

Let the two portions of a length $4N$ of the components of the bivariate process be obtained by the approach of Section 4.1 and stacked into two $4N$-dimensional vectors **X** and **Y**. We may write

$$\mathbf{X} \equiv \Pi^k \Omega^T \mathbf{U}, \tag{41}$$

$$\mathbf{Y} \equiv \Pi^k \Omega^T \mathbf{V}, \tag{42}$$

where the realization of the random variable k is the same in both the equations. **U** and **V** are two $4N$-dimensional zero-mean generating vectors. **U** is formed analogously to the way presented in Section 4.1, i.e., its elements are $4N$ independent random variables with the *unique* variances $2^1\alpha_{XX,1}, 2^2\alpha_{XX,2}, \ldots, 2^{J+2}\alpha_{XX,J+2}$ and $2^{J+2}\beta_{XX,J+2}$ set up in such a way so that the jth level (for $j = 1, \ldots, J + 2$) wavelet variances and the $(J + 2)$th level scaling variance of the first component are equal to $\eta_{XX,1}, \eta_{XX,2}, \ldots, \eta_{XX,J+2}$ and $\xi_{XX,J+2}$. **V** is constructed analogously, with the unique variances $2^1\alpha_{YY,1}, 2^2\alpha_{YY,2}, \ldots, 2^{J+2}\alpha_{YY,J+2}$ and $2^{J+2}\beta_{YY,J+2}$ of its elements set up in such a way so that the jth level (for $j = 1, \ldots, J + 2$) wavelet variances and the $(J + 2)$th level scaling variance of the second component are equal to $\eta_{YY,1}, \eta_{YY,2}, \ldots, \eta_{YY,J+2}$ and $\xi_{YY,J+2}$.

The second-order relationship between **X** and **Y** is described by the following cross-covariance matrix (see also Section 3.2):

$$\Sigma_{\mathbf{XY}} \equiv E\left(\mathbf{X}\mathbf{Y}^T\right) = circ\left(\Omega^T \Sigma_{\mathbf{UV}} \Omega\right), \tag{43}$$

where

$$\Sigma_{\mathbf{UV}} \equiv E\left(\mathbf{U}\mathbf{V}^T\right). \tag{44}$$

To ensure that the cross-covariance sequence between the components (of the bivariate process) is symmetric around zero, $\Sigma_{\mathbf{UV}}$ has to be symmetric. Moreover, based on the argument at the end of Section 3.2, the off-diagonal elements of $\Sigma_{\mathbf{UV}}$ can be set up equal to zero without losing much generality. As a result, we assume $\Sigma_{\mathbf{UV}}$ to be diagonal.

Let $\gamma_{XY,1}, \gamma_{XY,2}, \ldots, \gamma_{XY,J+2}$ and $\delta_{XY,J+2}$ be real-valued parameters, which can assume values from –1 (included) to 1 (included) and which are yet to be solved for (see Section 5.2) so that the prescribed scale-specific relationships are induced. The diagonal of $\Sigma_{\mathbf{UV}}$ consists of $2N + N + \ldots + 1 + 1 = 4N$ elements. Let the first N_1 elements of the diagonal be set equal to $2^1\gamma_{XY,1}(\alpha_{XX,1}\alpha_{YY,1})^{1/2}$, the next N_2 to $2^2\gamma_{XY,2}(\alpha_{XX,2}\alpha_{YY,2})^{1/2}$, …, the next N_{J+2} to $2^{J+2}\gamma_{XY,J+2}(\alpha_{XX,J+2}\alpha_{YY,J+2})^{1/2}$. Finally, let the last element of the diagonal be set equal to $2^{J+2}\delta_{XY,J+2}(\beta_{XX,J+2}\beta_{YY,J+2})^{1/2}$.

5.2 Obtaining the exact values of wavelet and scaling correlation

Following a similar line of argument to that of Section 4.2, we must set up the $(J + 3)$ values of the parameters $\gamma_{XY,1}, \gamma_{XY,2}, \ldots, \gamma_{XY,J+2}$ and $\delta_{XY,J+2}$ in such a way that the wavelet correlations between the components are equal to the required values $\rho_{XY,1}, \rho_{XY,2}, \ldots, \rho_{XY,J+2}$ and the $(J + 2)$th level scaling correlation to $\varphi_{XY,J+2}$. This can be achieved by solving an appropriate system of $(J + 3)$ linear equations for the values of the parameters $\gamma_{XY,1}, \gamma_{XY,2}, \ldots, \gamma_{XY,J+2}$ and $\delta_{XY,J+2}$. Since these parameters play the role of correlation coefficients, their values must lie in the range from –1 (included) to 1 (included) to be valid inputs into our methodology. Shall the solution to the system of linear equation not satisfy this constraint, it is not possible to simulate a bivariate process with the required wavelet and scaling variances and correlations.

5.3 The cross-covariance and cross-correlation sequence

Making use of Equation 43 and the partitioning of Ω given by Equation 3, we can write

$$\begin{aligned}\Sigma_{\mathbf{XY}} &= \sum_{j=1}^{J+2} 2^j \gamma_{XY,j}\sqrt{\alpha_{XX,j}\alpha_{YY,j}}\, circ(\Omega_j^T\Omega_j) + \\ &+ 2^{J+2}\delta_{XY,J+2}\sqrt{\beta_{XX,J+2}\beta_{YY,J+2}}\, circ(\Theta_{J+2}^T\Theta_{J+2}),\end{aligned} \tag{45}$$

which implies that $\Sigma_{\mathbf{XY}}$ is a sum of $(J + 3)$ matrices each associated with a specific scale. The cross-covariance sequence between $\{X_t: t = 0, \ldots, 4N - 1\}$ and $\{Y_t: t = 0, \ldots, 4N - 1\}$, denoted as $\{s_{XY,\tau}: \tau = -(4N - 1), \ldots, 0, \ldots, (4N - 1)\}$, can be extracted from $\Sigma_{\mathbf{XY}}$ as follows:

$$s_{XY,\tau} \equiv \begin{cases}\Sigma_{\mathbf{XY},|\tau|+1,1} & \text{for } \tau = -(4N-1),\ldots,-1,\\ \Sigma_{\mathbf{XY},1,\tau+1} & \text{for } \tau = 0,\ldots,(4N-1),\end{cases} \tag{46}$$

where $\Sigma_{\mathbf{XY},m,n}$ denotes the element of the matrix $\Sigma_{\mathbf{XY}}$ in the mth row and the nth column.

6. Illustration

Using our methodology, we generate two time series that might resemble (in some sense) time series of stock log returns, which are strongly negatively correlated on short scales and positively on long scales.

6.1 Setting of the simulation

We simulate a portion of a bivariate stationary stochastic process with zero-mean components. We use Haar wavelets and choose $J = 9$, which implies that $4N = 2^{J+2} = 2048$. Only the first N simulated values will be used for the final output. The univariate distribution of individual elements of the generating vectors **U** and **V** is normal.

The components of the simulated bivariate process are required to have the jth level wavelet variances (for $j = 1, \ldots, 11$) and the 11th level scaling variance in agreement with Table 1, which reports the 2^jth multiples of these characteristics. These scale-specific characteristics of variability are chosen in such a way so that both the components exhibit white noise behavior, the spectrum of both processes being constant and equal to unity. Consequently, the wavelet and scaling variances of both the processes are calculated based on the theory and formulas of Sections 3.3 and 3.1. Moreover, Table 1 also reports the jth level wavelet correlations (for $j = 1, \ldots, 11$) and the 11th level scaling correlation between the components. These characteristics of scale-specific relationships indicate a negative relationship on short scales and a positive one on long scales. For our setting of the parameters, we can also write $\rho_{XY,j} = 2^j \eta_{XY,j}$ (for $j = 1, \ldots, 11$) and $\varphi_{XY,11} = 2^{11} \xi_{XY,11}$.

If we solve for the values of the parameters $\alpha_{XX,1}, \alpha_{XX,2}, \ldots, \alpha_{XX,J+2}, \beta_{XX,J+2}$ and $\alpha_{YY,1}, \alpha_{YY,2}, \ldots, \alpha_{YY,J+2}, \beta_{YY,J+2}$ and $\gamma_{XY,1}, \gamma_{XY,2}, \ldots, \gamma_{XY,J+2}, \delta_{XY,J+2}$ (see Sections 5.1 and 5.2), we get the results given in Table 2 (again, 2^jth multiples are reported for convenience in some instances).

Table 1

The prescribed scale-specific characteristics of the simulated bivariate process. The 2^jth multiples of wavelet variances of both the components are reported together with wavelet correlations. The last column gives the prescribed values of $2^{11}\xi_{XX,11}$, $2^{11}\xi_{YY,11}$ and $\varphi_{XY,11}$.

4N=2048	*Haar wavelets*											
j	1	2	3	4	5	6	7	8	9	10	11	scal, 11
$2^j\eta_{XX,j}$	1	1	1	1	1	1	1	1	1	1	1	$2^{11}\xi_{XX,11} = 1$
$2^j\eta_{YY,j}$	1	1	1	1	1	1	1	1	1	1	1	$2^{11}\xi_{YY,11} = 1$
$\rho_{XY,j}$	-0.9	-0.9	-0.9	-0.9	-0.85	-0.6	0	0.4	0.65	0.8	0.85	$\varphi_{XY,11} = 0.95$

Table 2

The solved values of the parameters used as inputs to the simulation. The last column corresponds to $2^{11}\beta_{XX,11}$, $2^{11}\beta_{YY,11}$ and $\delta_{XY,11}$.

j	1	2	3	4	5	6	7	8	9	10	11	scal, 11
$2^j\alpha_{XX,j}$	1	1	1	1	1	1	1	1	1	1	1	$2^{11}\beta_{XX,11} = 1$
$2^j\alpha_{YY,j}$	1	1	1	1	1	1	1	1	1	1	1	$2^{11}\beta_{YY,11} = 1$
$\gamma_{XY,j}$	-0.9	-0.9	-0.89	-0.94	-0.97	-0.84	0.97	0.67	0.94	0.95	0.95	$\delta_{XY,11} = 0.95$

The theoretical autocovariance sequence (being the same for both the components) and the theoretical cross-covariance sequence, calculated making use of Equations 40 and 46, are plotted in Figure 1. The theoretical autocovariance sequence is non-zero only for the lag $\tau = 0$. The theoretical cross-covariance sequence exhibits a large negative peak at the lag $\tau = 0$ and is "slightly" non-zero also for other non-zero lags, which might be observed by noting a very small positive "bump" around the lag $\tau = 0$ in the right-hand plot of Figure 1.

Figure 1

The theoretical autocovariance sequence of both the components of the simulated bivariate process (left-hand plot, solid thick line) and the theoretical cross-covariance sequence between the components (right-hand plot, solid thick line). Thin vertical lines are plotted at the lag 0 and thin horizontal lines at the value of the autocovariance/cross-covariance equal to 0.

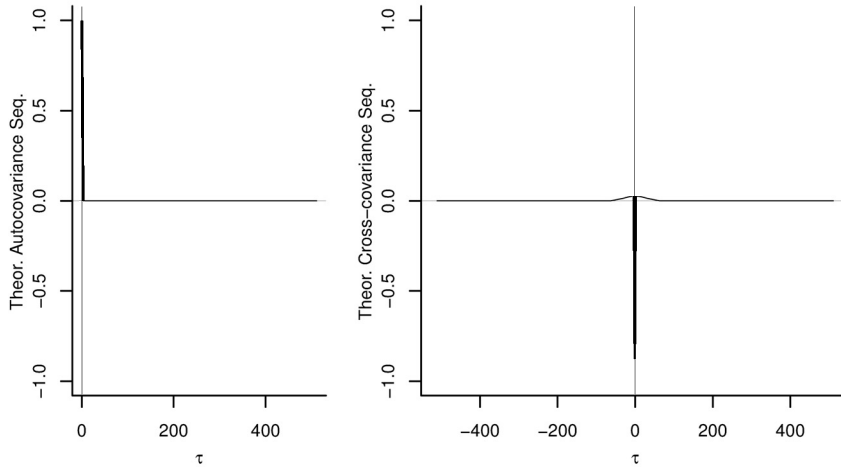

6.2 Monte Carlo simulation

To verify that our approach simulates the bivariate process with the prescribed scale--specific characteristics correctly, we run the simulation with the setting of Section 6.1 5000 times. For each simulation wavelet and scaling variances of the first component, wavelet and scaling covariances between the components, the autocovariance sequence

of the first component and the cross-covariance sequence between the components are estimated from the final output of length $N = 2^9 = 512$. The reason for not estimating the univariate characteristics of the second component stems from the fact that these are identical to those of the first component.

More specifically, the unbiased point estimates of $2^j\eta_{XX,j}$ (for $j = 1, \ldots, 9$), $2^9\xi_{XX,9}$, $2^j\eta_{XY,j}$ (for $j = 1, \ldots, 9$) and $2^9\xi_{XY,9}$ are calculated for each simulation. Afterwards, these estimates are averaged across the 5000 simulations. These averages are subtracted from the prescribed (theoretical) values, $2^j\eta_{XX,j}$ (for $j = 1, \ldots, 9$), $2^9\xi_{XX,9}$, $2^j\eta_{XY,j}$ (for $j = 1, \ldots, 9$) and $2^9\xi_{XY,9}$, and the differences are reported in Table 3 together with the estimates of the standard errors of the averages. The reason for estimating wavelet and scaling covariances rather than wavelet and scaling correlations is the fact that we can easily construct an unbiased estimate of wavelet and scaling covariance, which is not the case with estimating wavelet and scaling correlation[1].

The averages of estimates of $2^9\xi_{XX,9}$ and $2^9\xi_{XY,9}$ are reported in the last column of Table 3, being subtracted from the prescribed (theoretical) values of $2^9\xi_{XX,9}$ and $2^9\xi_{XY,9}$. However, the prescribed values of $2^9\xi_{XX,9}$ and $2^9\xi_{XY,9}$ are not available at the initial set up of the simulation (see Table 1). Fortunately, we can obtain $2^9\xi_{XX,9}$ and $2^9\xi_{XY,9}$ in terms of $\eta_{XX,10}$, $\eta_{XX,11}$, $\xi_{XX,11}$, $\eta_{XY,10}$, $\eta_{XY,11}$ and $\xi_{XY,11}$ (of Table 1), which cannot be estimated directly since the final output of the simulation is of a length N rather than $4N$. More specifically, it follows from Equation 28 and Section 3.3 that

$$\xi_{XY,9} = \xi_{XY,11} + \eta_{XY,10} + \eta_{XY,11} = 0.85 / 2^9 = \varphi_{XY,9} / 2^9, \tag{47}$$

$$\xi_{XX,9} = \xi_{XX,11} + \eta_{XX,10} + \eta_{XX,11} = 1 / 2^9. \tag{48}$$

The results of the Monte Carlo simulation suggest that our methodology simulates the bivariate processes with the required scale-specific characteristics correctly.

Table 3

The results of the Monte Carlo simulation (rounded). The last column reports the values of ($2^9\xi_{XX,9}$ – average est. of $2^9\xi_{XX,9}$) × 10^4, ($2^9\xi_{XY,9}$ – average est. of $2^9\xi_{XY,9}$) × 10^4 together with the respective estimates of standard errors of the averages.

j	1	2	3	4	5	6	7	8	9	scal, 9
($2^j\eta_{XX,j}$ – average est. of $2^j\eta_{XX,j}$) × 10^4	0	18	24	-54	-22	6	66	-110	270	-50
Est. of std. error of average × 10^4	12	18	25	36	50	70	98	140	210	200
($2^j\eta_{XY,j}$ – average est. of $2^j\eta_{XY,j}$) × 10^4	-2	-22	-15	32	23	-22	-36	-10	270	-20
Est. of std. error of average × 10^4	12	17	24	34	47	59	71	110	180	190

1 Unbiased estimators of wavelet and scaling variance and covariance can be easily constructed as traditional unbiased estimators of variance and covariance using non-boundary wavelet and scaling coefficients only.

Similarly, we calculate the sample autocovariance sequence of the first component and the sample cross-covariance sequence[2] for each of the 5000 simulations. Then, we calculate the average of the sequences across the 5000 simulations. These averages are subtracted from the theoretical sequences of Figure 1, the differences at individual lags being plotted in Figure 2 together with the estimates of the standard errors of the averages. Again, the results suggest that the true autocovariance and the true cross--covariance sequence of the simulated bivariate process are indeed identical to the theoretical ones of Figure 1.

Figure 2

Left-hand plot: The difference (thin line) between the average of the 5000 sample autocovariance sequences from the Monte Carlo simulation and the theoretical autocovariance sequence of Figure 1. Estimates of the standard errors of the average are plotted with the thick line. Right-hand plot: Analogously for the cross-covariance sequence.

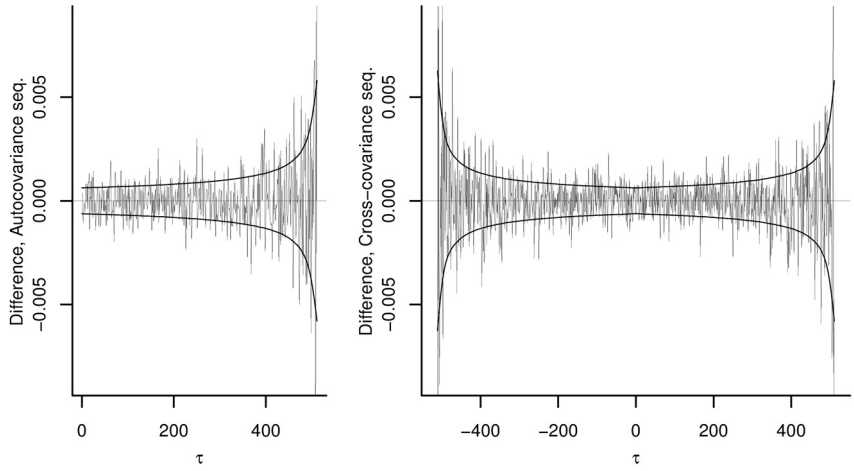

6.3 Examining one realization of the bivariate process

The left-hand plot of Figure 3 presents one realization of the bivariate process of the final length $N = 2^9$. Point estimates of $2^j\eta_{XX,j}$ (for $j = 1, \ldots, 9$) and $2^9\xi_{XX,9}$ and of $2^j\eta_{XY,j}$ (for $j = 1, \ldots, 9$) and $2^9\xi_{XY,9}$ are presented in Table 4. The sample autocovariance sequences of both the components and the sample cross-covariance sequence are presented in Figure 4.

To appreciate the importance of the positive relationship between the components on long scales, it is instructive to plot the cumulative sum of the values of both the

2 We assume that the means of the components are known to be zero. Under this assumption, we use the unbiased estimators of the true autocovariance and true cross-covariance sequences of the bivariate process to compute the sample autocovariance and sample cross-covariance sequences.

components – see the right-hand plot of Figure 3. The fact that the components (before they were cumulatively summed) appear to be simultaneously negatively correlated (as judged by the sample cross-covariance sequence of Figure 4) might suggest that the time series of the cumulative sums should move in opposite directions. However, this is true only for short time horizons, while in the long run these time series share the same direction, which is in agreement with the setting of the simulation.

Table 4

Point estimates of scale-specific characteristics of the simulated bivariate process calculated for the realization in the left-hand plot of Figure 3.

J	1	2	3	4	5	6	7	8	9	scal, 9
Est. of $2^j\eta_{XX,j}$	0.93	1.01	0.82	1.22	0.79	0.65	0.28	0.25	2.84	0.96
Est. of $2^j\eta_{YY,j}$	0.99	1.06	0.83	1.16	1.04	0.85	1.18	1.66	0.93	0.34
Est. of $2^j\eta_{XY,j}$	-0.87	-0.94	-0.74	-1.07	-0.83	-0.33	0.15	0.30	1.63	0.57

Figure 3

Left-hand plot: Simulation of the bivariate process with the prescribed scale-specific characteristics of Table 1. For the plotting purposes only, the realization of the second component is shifted by 7 units along the y-axis towards minus infinity. Right-hand plot: Sequences of cumulative sums.

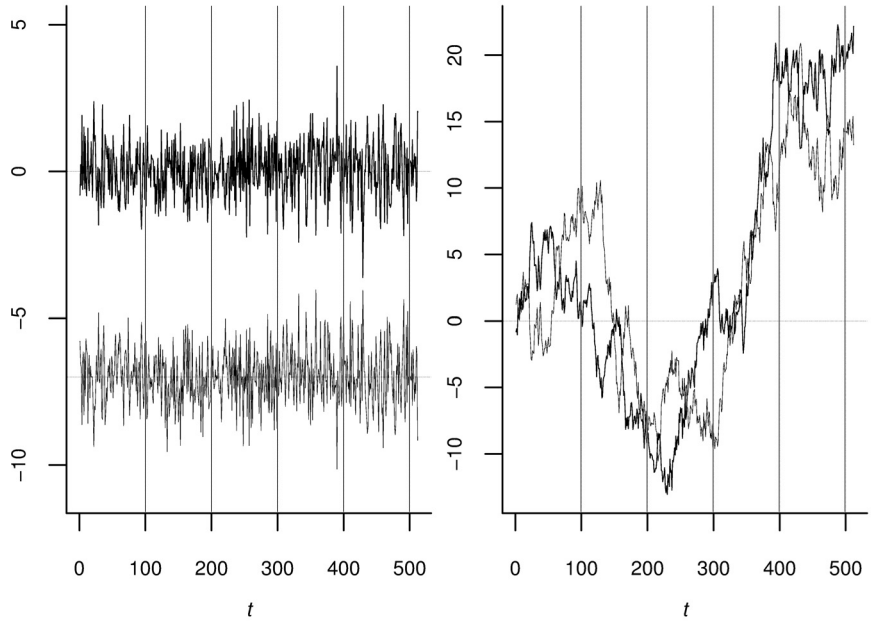

Figure 4

The sample autocovariance sequence of both components of the simulated bivariate process (top row, solid line) and the sample cross-covariance sequence between the components (bottom row, solid line). Thin vertical lines are plotted at the lag 0 and thin horizontal lines at the value of the autocovariance/cross-covariance equal to 0.

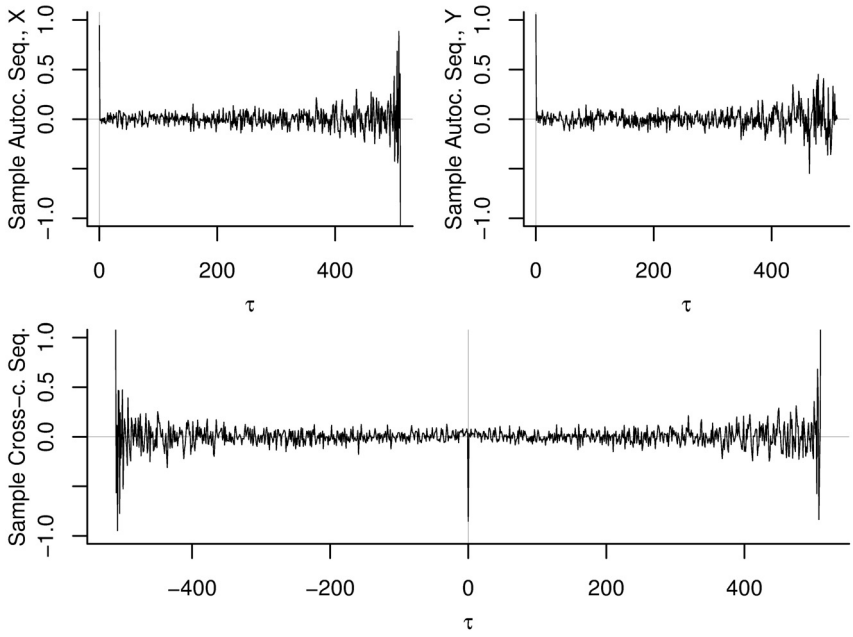

7. Comparison of our model with the literature

Equation 13 represents **X** in terms of **W**. Since Ω is orthogonal and thus invertible (Section 2.3), this representation is unique in the sense that, if **X** is given, the vector **W**, which satisfies Equation 13, is unique and given by Equation 1. Elements of **W** can be considered coordinates of **X** with respect to an orthonormal basis, the basis vectors being the columns of Ω^T and thus being associated with particular scales. The approach of the univariate simulation of Section 4 thus consists in reconstructing **X** from its coordinates ($\Omega\Pi^k\Omega^T\mathbf{U}$) with respect to the orthonormal basis (see Equation 35). Since the main diagonal of $\Omega_j^T\Omega_j$ is generally not constant, the univariate distribution of a given element of **X** is that of a mixture of Gaussians.

There are other flavors of wavelet transform such as the MODWT (see Percival and Walden, 2002), which projects **X** onto an overcomplete basis (frame), whose basis vectors are again associated with particular scales. While the use of the overcomplete basis leads to a non-unique representation of **X** in terms of the coordinates of **X** with respect to the overcomplete basis, its advantage lies in the fact that it provides a better way (when compared to the orthonormal basis of the DWT) of exploring "localized" structures in **X**, which can be useful for studying non-stationary time series. This is the

reasoning of Nason et al. (2000), who proposed a univariate locally stationary wavelet model based on an overcomplete basis.

The model of Nason et al. (2000) is primarily a model for univariate non-stationary time series with a time-varying autocovariance sequence. It can also be used to model univariate stationary time series with scale-specific characteristics of variability and for the simulation thereof. In that case, the simulated time series is reconstructed from the coordinates in the overcomplete basis; see Equation 7 of Nason et al., 2000. It follows from this equation that the simulated time series is necessarily Gaussian (as opposed to the non-Gaussian case of our model) if the joint distribution of the coordinates is multivariate normal. The autocovariance sequence of the simulated time series can be decomposed into so-called autocorrelation wavelets (see Nason et al., 2000, Section 2.3 and Equation 14). This decomposition is analogous to our decomposition of Equations 38 and 40.

Our simulation of the bivariate time series of Section 5 is a generalization of the univariate simulation of Section 4. Similarly, the model of Sanderson et al. (2010) is an extension of the locally stationary wavelet time series model of Nason et al. (2000) to the bivariate case. It aims at modeling non-stationary time series with a time-varying autocovariance and cross-covariance structure.

The models of Nason et al. (2000) and Sanderson et al. (2010) are supported with a well-developed theory and are generally more flexible when compared to our models of Section 4 and Section 5, since they can better handle time-varying second-order structures. On the other hand, since our models start from an orthonormal basis rather than an overcomplete one, their construction is more intuitive and may be more readily understood. The non-Gaussian nature of the simulated time series may also be convenient in some situations. Moreover, as a part of our models, we have also provided a way of obtaining simulated time series with exact scale-specific characteristics of variability and relationships.

8. Conclusion and discussion

We have modified and generalized the wavelet-based approach of Percival and Walden (2002), which was originally used for approximate simulation of univariate long--memory processes. More specifically, we proposed a methodology for simulating bivariate stationary processes exhibiting scale-specific relationships. Our simulation is exact in the sense that it achieves the required scale-specific characteristics. This was accomplished by solving a system of linear equations for several free parameters of the simulation. Using Monte Carlo simulation, we have verified that our methodology works correctly.

Our methodology might be suitable wherever scale-specific relationships are assumed to be present, which might possibly not be a scarce situation in finance and economics. This belief is supported by the fact that financial markets are formed by several groups of traders (market makers, intraday traders, hedge funds, portfolio managers, investment banks, etc.), which employ different tools of market analysis and have different information at hand, different risk profiles and trading preferences

and constraints. It can be argued that such differences among the groups might imply different time scales on which each group operates. Since each time scale is thus predominantly "operated" by a different group of traders with different characteristics, it can be expected that such a financial market, called the *heterogeneous market*, might exhibit different behavior on different scales (see also Zumbach and Lynch, 2001; Müller et al., 1993; Müller et al., 1997).

9. Acknowledgement

This paper was written at the Faculty of Informatics and Statistics, University of Economics in Prague, Czech Republic and was supported by the Czech Science Foundation (GA CR), grant no. P402/12/P507, Modelling of Financial and Economic Time Series – Application and Comparison of Wavelet and Traditional Methods. We also acknowledge the suggestions and comments of the reviewers, which helped us improve the paper.

References

ATKINS, F.; SUN, Z. Using wavelets to uncover the Fisher effect. [Discussion paper]. Department of Economics, University of Calgary, Canada, 2003.

GENÇAY, R.; SELÇUK, F.; WHITCHER, B.: Multiscale systematic risk. *Journal of International Money and Finance*. 2005, vol. 24, pp. 55-70.

McCOY, E.; WALDEN, A.: Wavelet analysis and synthesis of stationary long-memory processes. *Journal of Computational and Graphical Statistics.* 1996, vol. 5, p. 26-56.

MÜLLER, U.; DACOROGNA, M.; DAVÉ, R.; PICTET, O.; OLSEN, R.; WARD, J. Fractals and intrinsic time: A challenge to econometricians. Proceedings of the 39th International Conference of the Applied Econometrics Association on Real Time Econometrics, Luxembourg, 1993.

MÜLLER, U.; DACOROGNA, M.; DAVÉ, R.; OLSEN, R.; PICTET, O.; VON WEIZSÄCKER, J. Volatilities of different time resolutions – analyzing the dynamics of market components. *Journal of Empirical Finance.* 1997, vol. 4, p. 213-239.

NASON, G.; VON SACHS, R.; KROISANDT, G. Wavelet processes and adaptive estimation of the evolutionary wavelet spectrum. *Journal of the Royal Statistical Society: Series B (Statistical Methodology)*. 2000, vol. 62, pp. 271-292

PERCIVAL, D.; WALDEN, A. *Wavelet Methods for Time Series Analysis*. Cambridge University Press, 2002 (reprint). ISBN 9780521640687.

RAMSEY, J.; LAMPART, C: Decomposition of economic relationships by timescale using wavelets. *Macroeconomic Dynamics*. 1998a, vol. 2, pp. 49-71.

RAMSEY, J.; LAMPART, C. The decomposition of economic relationships by time scale using wavelets: expenditure and income. *Studies in Nonlinear Dynamics and Econometrics*. 1998b, vol. 3, p. 23-42.

SANDERSON, J.; FRYZLEWICZ, P.; JONES, M. Estimating linear dependence between nonstationary time series using the locally stationary wavelet model. *Biometrika*. 2010, vol. 97, p. 435-446.

SERROUKH, A.; WALDEN, A.: Wavelet scale analysis of bivariate time series I: motivation and estimation. *Journal of Nonparametric Statistics*. 2000a, vol. 13, p. 1-36.

SERROUKH, A.; WALDEN, A. Wavelet scale analysis of bivariate time series II: statistical properties for linear processes. *Journal of Nonparametric Statistics*. 2000b, vol. 13, pp. 37-56.

VIDAKOVIC, B. *Statistical Modeling by Wavelets*. Wiley-Interscience, 1999. ISBN 9780471293651.

WHITCHER, B.; GUTTORP, P.; PERCIVAL, D. Mathematical background for wavelet estimators of cross--covariance and cross-correlation. [National Research Center for Statistics and the Environment Technical Report Series]. 1999, vol. 38.

WHITCHER, B.; GUTTORP, P.; PERCIVAL, D. Wavelet analysis of covariance with application to atmospheric time series. *Journal of Geophysical Research: Atmospheres (1984-2012)*. 2000, vol. 105, p.14941-14962.

WORNELL, G. Wavelet-based representations for the 1/f family of fractal processes. Proceedings of the IEEE, 1993, vol. 81, pp. 1428-1450

WORNELL, G: *Signal processing with fractals: a wavelet-based approach*. Upper Saddle River, New Jersey : Prentice Hall, 1996.

ZUMBACH, G.; LYNCH, P. Heterogeneous volatility cascade in financial markets. *Physica A: Statistical Mechanics and its Applications.* 2001, vol. 298, p. 521-529.

SIMULATING BIVARIATE STATIONARY PROCESSES WITH SCALE-SPECIFIC CHARACTERISTICS

Abstract: By modifying and generalizing the wavelet-based approach of approximately simulating univariate long-memory processes that is available in the literature, we propose a methodology for simulating a bivariate stationary process, whose components exhibit different relationships at different scales. We derive the formulas for the autocovariance and cross-covariance sequences of the simulated bivariate process. We provide a setting for the parameters of the simulation which might generate a bivariate time series resembling that of stock log returns. Using this setting, we study the properties of our methodology via Monte Carlo simulation.

Keywords: time series, bivariate, wavelets, finance

JEL Classification: C49, C32, C53, C58, G10